

Journal Pre-proof

Crustal deformation in the Rio de la Plata estuarine (South Atlantic passive margin) and the associated seismicity as a consequence of an isostatic readjustment

Laura Godoy, Mario E. Gimenez, Silvina Nacif, Orlando Alvarez, Andrés Folguera



PII: S0895-9811(20)30313-8

DOI: <https://doi.org/10.1016/j.jsames.2020.102770>

Reference: SAMES 102770

To appear in: *Journal of South American Earth Sciences*

Received Date: 10 May 2020

Revised Date: 15 July 2020

Accepted Date: 15 July 2020

Please cite this article as: Godoy, L., Gimenez, M.E., Nacif, S., Alvarez, O., Folguera, André., Crustal deformation in the Rio de la Plata estuarine (South Atlantic passive margin) and the associated seismicity as a consequence of an isostatic readjustment, *Journal of South American Earth Sciences* (2020), doi: <https://doi.org/10.1016/j.jsames.2020.102770>.

This is a PDF file of an article that has undergone enhancements after acceptance, such as the addition of a cover page and metadata, and formatting for readability, but it is not yet the definitive version of record. This version will undergo additional copyediting, typesetting and review before it is published in its final form, but we are providing this version to give early visibility of the article. Please note that, during the production process, errors may be discovered which could affect the content, and all legal disclaimers that apply to the journal pertain.

© 2020 Published by Elsevier Ltd.

"CRUSTAL DEFORMATION IN THE RIO DE LA PLATA ESTUARINE (SOUTH ATLANTIC PASSIVE MARGIN) AND THE ASSOCIATED SEISMICITY AS A CONSEQUENCE OF AN ISOSTATIC READJUSTMENT".

Godoy Laura^{1*}; Gimenez Mario E¹; Nacif Silvina¹; Alvarez Orlando¹; Folguera Andrés².

¹ Instituto Geofísico Sismológico Volponi. FCFN. Universidad Nacional de San Juan. CONICET. Ruta 12 km 17. Marquesado, Rivadavia. San Juan. CP 5400.

² Instituto de Estudios Andinos. *Don Pablo Groeber*. UBA – CONICET

Corresponding author: * laurabeatrizgodoy@gmail.com

ABSTRACT

The Río de la Plata estuarine has been the epicenter of the 30 November 2018 intra-crustal earthquake with a magnitude and focal depth of 3.7 and 19 km (± 6 km), respectively, which alerted the Buenos Aires city population. This area has also been the locus of a series of earthquakes with magnitudes ranging from 3.7 to 5, and particularly the 1888 earthquake, probably with an epicenter near the axis of the estuarine. These earthquakes occur in the Salado basin area, an aulacogen basin associated with the early stages of the South Atlantic spreading in late Early Cretaceous times, that subsided all through the Cenozoic. Previous gravimetric analyses revealed that this basin is characterized by an important crustal attenuation zone. From a new gravimetric analysis, using satellite gravity data, we find isostatic anomalies associated with this section of the Atlantic passive margin. Therefore, we propose that the origin of these earthquakes is the isostatic readjustment of this aulacogen type basin, a process that could have reactivated shallow crustal structures. From a preliminary evaluation, we estimate that the Salado basin would subsidize other ~ 2 km to compensate for the measured thick anti-root, constituting a crucial seismogenic source that should be considered due to the demographical and economic importance of the region.

Keywords: Seismicity, Passive Margin, Tectonics, Satellite Gravity

INTRODUCTION

In the Argentine continental margin, the aulacogen type Salado basin was associated with the early stages of the South Atlantic, spreading from 115 Ma onwards (e.g., Barredo and Stinco, 2010).

This basin has been widely studied, mainly for economic proposes, and also because it presents a significant positive value of Bouguer anomaly (e.g., Croveto et al., 2007). From terrestrial gravimetric data, Introcaso (1980) and Introcaso (1997) found a relevant anti root, which cannot be entirely compensated with the sedimentary column load considering the Airy hypothesis. More recently, Croveto et al. (2007), from gravity anomalies and geoid undulations, studied this basin detecting through both techniques a gravity high located in the basin, which was also interpreted as a significant anti root. Mukherjee (2017) presented a more refined Airy isostasy model taking into account variation of density in three dimensions. However, such a refined model applied for the study area is not valid.

Notably, this region was the location of the 30 November 2018 earthquake with a magnitude and focal depth of 3.7 and 19 km (± 6 km), respectively (Venerdini et al., 2019).

From CERESIS Catalog (Catálogo del Centro Regional de Sismología para América del Sur) and NEIC catalog (1998), evidence of several earthquakes occurring since 1845 can be collected, with magnitudes ranging from 3.7 to 5.

Cappellotto et al. (2020), using high-precision geodetic techniques and geological data, determined that sea-level would have descended in the Salado basin 4 meters since the late Pleistocene based on outcrops of the marine Belgranense deposits.

In this work, we evaluate through satellite gravity data a possible link between crustal seismicity recorded for this region and an isostatic readjustment of the Salado basin

GEOLOGICAL SETTING

An extensive Quaternary sedimentary cover develops over the Atlantic passive margin at the latitude of the Buenos Aires Province plain in Argentina. Its origin is associated

with several sublithospheric and lithospheric processes, from dynamic subsidence at the leading edge of the Chilean-Pampean flat subduction zone (Dávila et al., 2010), to subsidence in the back bulge depocenter zone in a flexural basin associated with the Andes (Nivière et al., 2013). Beneath this sedimentary plain, a complex structure is linked to the early evolution of the passive Atlantic margin. This structure comprises two aulacogen type basins, the Salado and Colorado basins, that dispose perpendicularly of respect to the Atlantic passive margin (Figure 1). These taphrogenic basins are associated with inflections of the margin that are controlling syn-extensionally late Early Cretaceous sedimentary series equivalent to those deposited in the adjacent passive margin (see Ramos et al. 1984). These Early Cretaceous sedimentary series are interfingered with mafic materials at the axes of the extensional depocenters revealed by gravity lows (Introcaso, 1980). Subsequently, progressively wider depocenters expanded through the Paleogene and Neogene, forming symmetrical sag deposits elongated over the WNW predominant syn-rift geometries.

The first geophysical studies made along the Salado basin were performed by Yacimientos Petrolíferos Fiscales (YPF), including twelve exploration boreholes made over the basin drilled by YPF and by other hydrocarbon exploration companies. Several seismic profiles reveal basement depths up to 7000 m in the depocentre. The Cretaceous sedimentary Salado basin sequence lays unconformably over a Precambrian and Paleozoic basement and covers partially or interfingers with Upper Jurassic-Lower Cretaceous basaltic flows. At the base, this sequence contains about 3500 m of reddish, brown, and purple cross-bedded continental sandstones and claystones of the Rio Salado Formation. Drills have reached ~2000 m in these syn-extensional deposits that contain a microflora no older than Aptian (Zambrano, 1974; Yrigoyen, 1975b). The Rio Salado Formation is overlain unconformably by 890 m of coarser reddish, greenish continental sandstones intercalated with claystones and conglomerates (Tavella and Wright, 1996).

Martin (1954), Orellana (1964), Introcaso (1980), Introcaso (1997a), applying gravity data, highlighted the positive gravity response obtained through the axis of the basin.

Latter, Introcaso et al. (2002) make use of geoid undulations to study the Salado Basin, refining the area of positive gravity anomalies. More recently, Croveto et al. (2007) proposed a stretching model in perfect Airy isostatic balance to explain the Salado Basin.

Concerning the record of seismic activity, Venerdini et al. (2019) presented the focal mechanism solution for the 30 November 2018 earthquake, associating this event with a dominant strike-slip component (with an associated inverse component). Its displacement had West-Northwest (W-NW) strike, most likely related to the Paraná Fault System, which runs through the homonymous fluvial basin to the north of Buenos Aires city.

GRAVITY MODEL

We applied the gravity model EIGEN 6C4 (Förste et al., 2014), from Global Gravity Field Models (http://icgem.gfz-potsdam.de/tom_longtime). This model is based on a set of spherical harmonic coefficients involved in a global database of terrestrial, marine, and aerial gravity anomalies, up to a degree and maximum order (N_{\max}). The maximum degree and order reached by the model are $N = 2159$, with some additional terms up to the degree and order 2190. The model spatial resolution λ depends on the maximum degree N_{\max} (Li, 2001; Hofmann-Wellenhof and Moritz, 2006; Barthelmes, 2009); in this way, the relationship between the degree of development in spherical harmonics N and the smallest gravity field characteristic observable is equal to 9 km ($\lambda / 2$).

We regularized the data in a regular grid with a cell size of 0.05° , in a geocentric spherical coordinate system at the height of 4,000 m to ensure that all values were above the topography, and was corrected by this effect to eliminate its influence.

For the topographic corrections, we used the ETOPO1 model (Amante and Eakins, 2008) and represented with constant density spherical prisms in spherical coordinates (Alvarez et al., 2013b; Bouman et al., 2013; Uieda et al., 2015). A standard density of 2670 kg/m^3 was considered (Hinze, 2003), for the continental rocks and 1030 kg/m^3 for seawater. All calculations were incorporated in the WGS84 model (World Geodetic

System, 1984). In Figure 2, the anomaly chart corrected by the topographic effect is presented.

MOHO DEPTH FROM GRAVITY INVERSION

We used the model of Moho obtained by Uieda and Barbosa (2017), based on satellite-derived gravity and seismological data. This model combines the highly efficient Bott's method with smoothness regularization and a discretization of the anomalous Moho into tesseroids (spherical prisms). Moho depths are estimated for the entire South American continent using the corrected gravity anomaly and seismological data sets (Assumpção et al., 2013), which were used for the validation of the inversion model. These authors obtained the gravity anomaly from the Earth gravity field model GOCO5S (Mayer-Guerr, 2015) by removing: (I) the normal gravity, (II) the gravitational effect of the topography and basins infills. Corrections were calculated by modeling the ETOPO1 digital terrain model (Amante and Eakins, 2008) and the CRUST1.0 model (Laske et al., 2013), using tesseroids and a standard density of 2670 for continents and -1630 kg/m^3

for the oceans (detail in Silva et al., 2014; Uieda and Barbosa, 2017).

The inversion model was controlled by three hyperparameters: i) the regularization parameter estimated by the method of holdout cross-validation; ii) the anomalous Moho density contrast, and iii) the reference Moho depth; being the last two estimated using the knowledge of the Moho depth at control points (for more details, see Uieda and Barbosa, 2017).

ISOSTASY

Seismic studies show that Airy's model explains variations in the structure of the crust associated with surfaces such as mountains and continental margins (Watts, 2001). For the tectonic style that the aulacogen type basin of Salado presents, we applied local isostasy.

The isostatic anomaly was computed, where isostatic compensation is complete and local.

That is, the mass column is compensated directly below a certain level of compensation.

The crust and mantle densities are assumed constant, and the crust takes the value of 35 km as the normal thickness of the crust. We consider that the topography mass excess is balanced by replacing mantle material with relatively lower density material in the form of a crustal root. To calculate the isostatic anomaly, we used the following parameters: a topographic density of 2670 kg/m^3 , a water density of 1030 kg/m^3 , a density contrast between crust and mantle of 400 kg/m^3 , and a normal crustal thickness of 35 km according to seismological studies (Assumpção et al., 2013). We averaged the ETOPO1 model using a grid with a cell size of $10 \times 10 \text{ km}^2$ without a low-pass pre-filter. The Bouguer anomaly corrected by sediments was compared with the Moho gravity effect calculated according to Introcaso (1997), to obtain the isostatic anomaly.

DECOMPENSATED ISOSTATIC RESIDUAL ANOMALY

Gravity anomalies generated from geological structures placed in the upper crust are contaminated by deeper sources. Isostatic corrections (e.g., Cordell et al. 1991) can be used to remove, in part, the effect of crustal roots produced by topographic highs and lows. Still, they do not solve the problem when crustal roots derive from regions with high crustal density with or without topographic expression. Isostatic decompensation correction (Cordell et al., 1991) is an approach to compensate or counteract this effect.

Considering that the anomalies contained in the prolonged field at a certain height (in this case at 40 km altitude) must have an origin at the lower and upper mantle, the correction for isostatic decompensated is calculated from an ascending prolongation of the isostatic anomaly (UP 40KM [AI]). This regional anomaly is subtracted from the isostatic anomaly (AI) to obtain the isostatic decompensated anomaly (DA).

$$DA = AI - UP40km [AI] \quad (1)$$

Figure 5 shows the isostatic residual, topography, sedimentary thickness, and Moho for cross-section A-B (Figure 1), to visualize the first results in a cross-section cutting through the middle of the Salado basin. This cross-section is located in the middle part

of the Salado basin with a longitude of 120 km in Southwest-Northeast direction (SW-NE).

STATE OF EQUILIBRIUM OF THE CRUST AT THE SALADO BASIN

Schematically in Figure 6, we represent the Moho geometry below the Salado basin and its sediments thickness. The Moho deflects upward into the lower crust at 28 km (Figure 3) with respect to the normal thickness of the crust (assumed in 35 km). The sediment prism gets a maximum depth of 3.5 km (Crovetto et al., 2007), while the calculated Anti-root (ΔR) = (T_n - Moho) = 7 km (considering a Sediment Density (σ_s) = 2350 kg/m³; Crust Density (σ_c) = 2900 kg/m³; Mantle Density (σ_m) = 3300 kg/m³). Thus, the following equation provides the averaged subsidence (X) to achieve the basin re-balance:

$$(SB + X) * (\sigma_c - \sigma_s) = ((T_n - \Delta R) - X) * (\sigma_m - \sigma_c) \quad (2)$$

Realign:

$$X = (T_n - \Delta R) * (\sigma_m - \sigma_c) - SB * (\sigma_c - \sigma_s) / (\sigma_c - \sigma_s) + (\sigma_m - \sigma_c) \quad (3)$$

Replacing the values in the equation (3), we get that the Salado basin would need to subside $X = 2.1$ km, to balance its anti-root.

In Figure 7, we present a 3D model where the different charts shown in this work are integrated. This allows us to visualize the anti-root in the Moho chart and the effects it causes.

RESULTS AND DISCUSSION

The Bouguer anomaly map (Figure 2) shows a range of values from -70 mGal to +70 mGal. The maximum values are located at the Argentine continental shelf, and the minimum values mainly located in the western region and linked to the highest topography. In the central zone, the Claromecó basin is observed with negative gravity responses, which underestimate with its negative gravity effect, the positive gravimetric values of the Paleozoic rocks exposed at La Ventana range (Figure 1). In the Colorado and the Salado basins, similar gravity values are observed (-25 mGal and +25

mGal, respectively) (Figure 2), related to an important gravimetric effect in response to the anti-roots of these basins, minimizing the gravity effect of the sedimentary columns. . The seismicity reported for this region (Table 1) is mostly located in the Salado basin area and at a depth of 19 km (± 6 km), considering the most reliable hypocenter determination. As regards the crustal thickness of this region, the Moho depth varies from ~ 27 km to 30 km (Figure 3), which is consistent with the focal depth of the 2018 earthquake obtained by Venerdini et al. 2019.

In order to analyze the anomaly of the shallowest effect at the Salado basin, the isostatic anomaly was calculated (in the concept of Airy) and, subsequently, the isostatic residual anomaly. In both cases, a clear isostatic overcompensation is observed, as previous works had indicated (Introcaso 1980, Introcaso 1997a, Introcaso et al., 2002; and Croveto et al., 2007).

The Salado basin must experience subsidence of approximately 2.1 km to compensate for the anti-root effect (for detail, see the previous section). According to this hypothesis, the main movements in this region should be downward.

Co-seismic and post-seismic horizontal gradient velocity fields in giant subduction-related earthquakes, as the Maule 2010 Mw 8.8 earthquake, have been measured up to the Atlantic coast (e.g., Klein et al. 2016, Brunetto et al., 2017).

The strike-slip solution with an inverse component for the 30 November 2018 event determined by Venerdini et al. (2019) could indicate the existence of horizontal stresses at the Atlantic passive margin area that could act superposed to subsidence (isostatic) dynamics. However, that result loses weight considering that the GAP (maximum azimuthal angle between adjacent stations) exceeds 90° , which can introduce instabilities in the focal mechanism solutions (e.g., Hardebeck and Shearer, 2002).

The 2018 earthquake is the most constrained located event, of a series of events located in the Río de la Plata basin area, and its epicenter is situated on the edge of the Salado basin. This is consistent with the subsidence of the basin, considering that at the edges is where the highest tension occurs, which would promote brittle deformation.

CONCLUSIONS

We analyzed from the gravity point of view the seismicity reported in the region of the aulacogen type Salado basin, with a high population density and economic importance. A significant anti-root is detected from its gravity effect that overlaps that of the sediments. This region is characterized by low to moderate magnitude historical earthquakes. The 30 November 2018 earthquake falls in this same category with similar spatial localization, depth and magnitude. We interpret the origin of this seismicity as mainly related to a regional readjustment, in which the Salado basin would need to subside another 2.1 km to reach isostatic equilibrium. However, co- and post-seismic stresses acting superimposed to subsidence mechanisms cannot be discarded as triggerings of this seismicity.

Acknowledgments:

The authors would like to thank the Consejo Nacional de Ciencia y Técnica (CONICET) for financial support through PIP 2016-2019 and the Universidad Nacional de San Juan. We also especially want to thank Soumyajit Mukherjee (IIT Bombay), for his valuable contribution made that allowed us to improve the manuscript.

REFERENCES

- Alvarez, O., Gimenez, M., Braitenberg, C. 2013. Nueva metodología para el cálculo del efecto topográfico para la corrección de datos satelitales. *Revista de la Asociación Geológica Argentina*, 70, 499-506.
- Amante, C., Eakins, B.W. 2009. ETOPO1 1 Arc-Minute Global Relief Model: Procedures, Data Sources and Analysis. NOAA Technical Memorandum NESDIS NGDC-24. National Geophysical Data Center, NOAA. doi:10.7289/V5C8276M.
- Assumpção, M., Feng M., Tassara A., Julià J., 2013. Models of crustal thickness for South America from seismic refraction, receiver functions and surface wave tomography. *Tectonophysics*, 609, 82-96.

- Barredo, S. Stinco, L. 2010. Geodinámica de las cuencas sedimentarias: su importancia en la localización de sistemas petroleros en la Argentina. *Petrotecnia* 48-68.
- Barker, P. 1982. Tectonic Evolution and Subsidence History of The Rio Grande Rise. In Barker, P. R, Carlson, R. L., Johnson, D. A., et al., *Init. Repts. DSDP, 72: Washington (U.S. Govt. Printing Office): 953-976.*
- Barthelmes, F. Kohler, W. (2016), International Centre for Global Earth Models (ICGEM), in: Drewes, H., Kuglitsch, F., Adam, J. et al., *The Geodesists Handbook 2016, Journal of Geodesy (2016), 90(10), 907-1205, doi:10.1007/s00190-016-0948-z*
- Bouman, J., Ebbing, J. Fuchs, M. 2013. Reference frame transformation of satellite gravity gradients and topographic mass reduction. *Journal of Geophysical Research, Solid Earth* 118, 759-774.
- Brunetto, E., et al., Quaternary deformation and stress field in the Río de la Plata Craton (Southeastern South America), *Journal of South American Earth Sciences* (2017), <http://dx.doi.org/10.1016/j.jsames.2017.04.010>.
- Cappellotto, L., A. M.C. ACOSTA, D. J. PÉREZ, M. J. ORGEIRA y D. GÓMEZ, 2020. Determinación de alta precisión de la altura del nivel del mar alcanzada por la ingresión Belgranense para el sector norte de Buenos Aires y sur de Santa Fe y Entre Ríos. *Revista de la Asociación Geológica Argentina* 77 (1): 132-143.
- Cordell L., Zorin, Y.A., Keller, G.R. 1991. The Decompensative Gravity Anomaly and Deep Structure of the Region of the Rio Grande Rift. *Journal of Geophysical Research*, Vol. 96, 6557-6568.
- Crovetto, C.; Novara, I.L., Instrocaso, A. 2007. A Stretching Model to Explain the Salado Basin (Argentina). *Boletín del Instituto de Fisiografía y Geología* 77(1-2).
- Dávila, F., C. Lithgow-Bertelloni, M. E. Gimenez. 2010. Tectonic and Dynamic Controls on the Topography and Subsidence of the Argentine Pampas: The role of the Flat Slab. *Earth and Planetary Science Letters*, 295: 187-194.
- Förste, Christoph; Bruinsma, Sean.L.; Abrikosov, Oleg; Lemoine, Jean-Michel; Marty, Jean Charles; Flechtner, Frank; Balmino, G.; Barthelmes, F.; Biancale, R., 2014: EIGEN-6C4 The latest combined global gravity field model including GOCE data up to degree and order 2190 of GFZ Potsdam and GRGS Toulouse. GFZ Data Services. doi:10.5880/icgem.2015.1

- Hardebeck, J., Shearer, P., 2002. A new method for determining first motion focal mechanisms. *Bull. Seismol. Soc. Am.* 92 (6), 2264– 2276.
- Hinze, W. Bouguer reduction density, why 2.67?. 2003. *Geophysics*, 68, 5:1559–1560
10.1190/1.1620629
- Hofmann-Wellenhof, B., & Moritz, H. (2006). *Physical Geodesy* (2nd, corr. ed. 2006 edition ed.). Wien ; New York: Springer.
- Introcaso A., 1980. A gravimetric interpretation of the Salado Basin (Argentina). *Bollettino di Geofisica Teorica ed Applicata* 22(87): 187-200.
- Introcaso A., 1997a. *Gravimetría*. UNR Editora, 359 pp., Rosario.
- Introcaso A., 1997b. La evolución futura de la cuenca del Salado. Tesis Doctoral Universidad Nacional de Rosario, 150 pp., Rosario.
- Introcaso A. y Ramos V., 1984. La cuenca del Salado. Un modelo de evolución aulacogénica. *Noveno Congreso Geológico Argentino (Bariloche)* 3: 27-46.
- Introcaso A., Guspí F. e Introcaso B., 2002. Interpretación del estado isostático de la Cuenca del Salado (Provincia de Buenos Aires) utilizando un geoide local obtenido mediante fuentes equivalentes a partir de anomalías de aire libre. *Actas del Decimoquinto Congreso Geológico Argentino (El Calafate)*. Artículo 139, 6 pp.
- Klein, E., Fleitout, L., Vigny, C. y Garaud, J. 2016. Afterslip and viscoelastic relaxation model inferred from the large-scale post-seismic deformation following the 2010 Mw 8.8 Maule earthquake (Chile). *Geophysical Journal International*, 205(3): 1455-1472.
- Laske G., Masters G., Ma Z., Pasyanos M., 2013. Update on CRUST1.0—1-degree Global Model of Earth's Crust, in *EGU General Assembly Conference Abstracts*, vol. 15, pp. EGU2013–2658.
- Lesta P., 1974. Exploraciones de la Patagonia Continental Argentina. *Comunicación yacimientos Petrolíferos Fiscales (Buenos Aires)* 8: 20 -41.
- Martin R., 1954. Gravity Maxima corresponding with sedimentary basins. *Geophysics* 19: 89-94.

- Mayer-Guerr T. et al., 2015. The combined satellite gravity field model GOCO05s, in EGU General Assembly Conference Abstracts, vol. 17, pp. EGU2015, 12364.
- Mukherjee S. (2017) Airy's isostatic model: a proposal for a realistic case. *Arabian Journal of Geosciences* 10: 268.
- Nivière, B., G. Messenger, S. Carretier, P. Lacan. 2013. Geomorphic expression of the southern Central Andes forebulge (37°S, Argentina). *Terra Nova* 25, 361–367. DOI: 10.1111/ter.12044
- Orellana E., 1964. Contribución al conocimiento de la corteza terrestre bajo la cuenca sedimentaria del río Salado. Tercera Reunión Asociación Argentina de Geofísicos y Geodestas (Rosario), 53 pp.
- Pavlis, N.K., Holmes, S.A., Kenyon, S.C. y Factor, J.K. 2012. The development and evaluation of the Earth Gravitational Model 2008 (EGM2008), *Journal of Geophysical Research* 117, B04406.
- Perdomo R. & Del Cogliano D., 1999. The geoid in Buenos Aires region. *International Geoid Service, Bulletin, Special Issue for South America* 9: 109-116.
- Silva, J., Santos, D., & Gomes, K., 2014. Fast gravity inversion of basement relief, *Geophysics*, 79(5), G79– G91.
- Tavella G. & Wright C., 1996. Cuenca del Salado. Decimotercero Congreso Geológico Argentino y Tercer Congreso de Exploración de Hidrocarburo, Buenos Aires. In: V.A. Ramos, M.A.Turic (eds.): *Geología y Recursos Naturales de la Plataforma Continental Argentina*, Relatorio 6: 95-116.
- Uieda L., 2015. A tesseroid (spherical prism) in a geocentric coordinate system with a local North-oriented coordinate system, figshare, Available at: <https://dx.doi.org/10.6084/m9.figshare.1495525.v1>.
- Uieda, L., and V. C. F. Barbosa (2017), Fast nonlinear gravity inversion in spherical coordinates with application to the South American Moho, *Geophysical Journal International*, 208(1), 162-176, doi:10.1093/gji/ggw390
- Uliana. M. A., Biddle, K. T., Cerdan, J., 1989. Mesozoic extension and the formation of the Argentina Sedimentary Basins. In Tankard, A. J., Balkwill, H.R., (editors):

- Extensional Tectonics and Stratigraphy of the North Atlantic Margins. American Association of Petroleum Geologists, Memoria 46, 599-613 p.
- Urien, C.M. y Zambrano, J.J., 1996. Estructura de la Plataforma Continental Argentina. In Ramos, V.A. and Turic, M.A. (editors): Geología y Recursos Naturales de la Plataforma Continental Argentina. XIII Congreso Geológico Argentino y XXXI Congreso de Exploración y Desarrollo de Hidrocarburos. Relatorio, 29-66 p.
- Venerdini, A.; López, L.; Orozco, P.; Sánchez, G.; Alvarado, P., Perucca, L., Galván, R., 2019. Parametrización Sismológica del Sismo del 30 de noviembre de 2018, Buenos Aires, Argentina. Revista de la Asociación Geológica Argentina 76 (3): 173-182.
- Watts, A.B. 2001. Isostasy and Flexure of the Lithosphere. Cambridge University Press. 451p. ISBN 0 521 62272 7.
- Yrigoyen, M. R. 1975b. Geología del Subsuelo y Plataforma Continental. Geología de la Provincia de Buenos Aires, VI Congreso Geológico Argentino, Relatorio, 139-168, Bs. As.
- Zambrano J.J., 1974. Cuencas Sedimentarias en el subsuelo de la provincia de Buenos Aires y zonas adyacentes. Revista de la Asociación Geológica Argentina 29(4): 443-449.

FIGURE CAPTIONS

Figure 1: Basins of the eastern central region of Argentina (Black dotted lines polygons). Crustal seismicity (red stars) reported for the Salado basin and surrounding regions (CERESIS, NEIC, Venerdini et al., 2019). The black line shows the cross-section (A-B) in Figure 5.

Figure 2: Bouguer anomaly obtained from EIGEN 6C4 model (Förste, et al., 2014), corrected for topographic effect. Red stars represent seismic events reported by the CERESIS catalog, NEIC catalog and Venerdini et al., 2019.

Figure 3: Moho model from Uieda and Barbosa (2017) with a density contrast of 400 kg/m^3 and a reference level at 35 km. Red stars represent seismic events reported by the CERESIS catalog NEIC catalog and Venerdini et al., 2019.

Figure 4: Decompensated isostatic residual anomaly map based on Cordel et al. (1991). The main geological structures were plotted on it and the red stars represent seismic events reported by the CERESIS catalog, NEIC catalog and Venerdini et al., 2019.

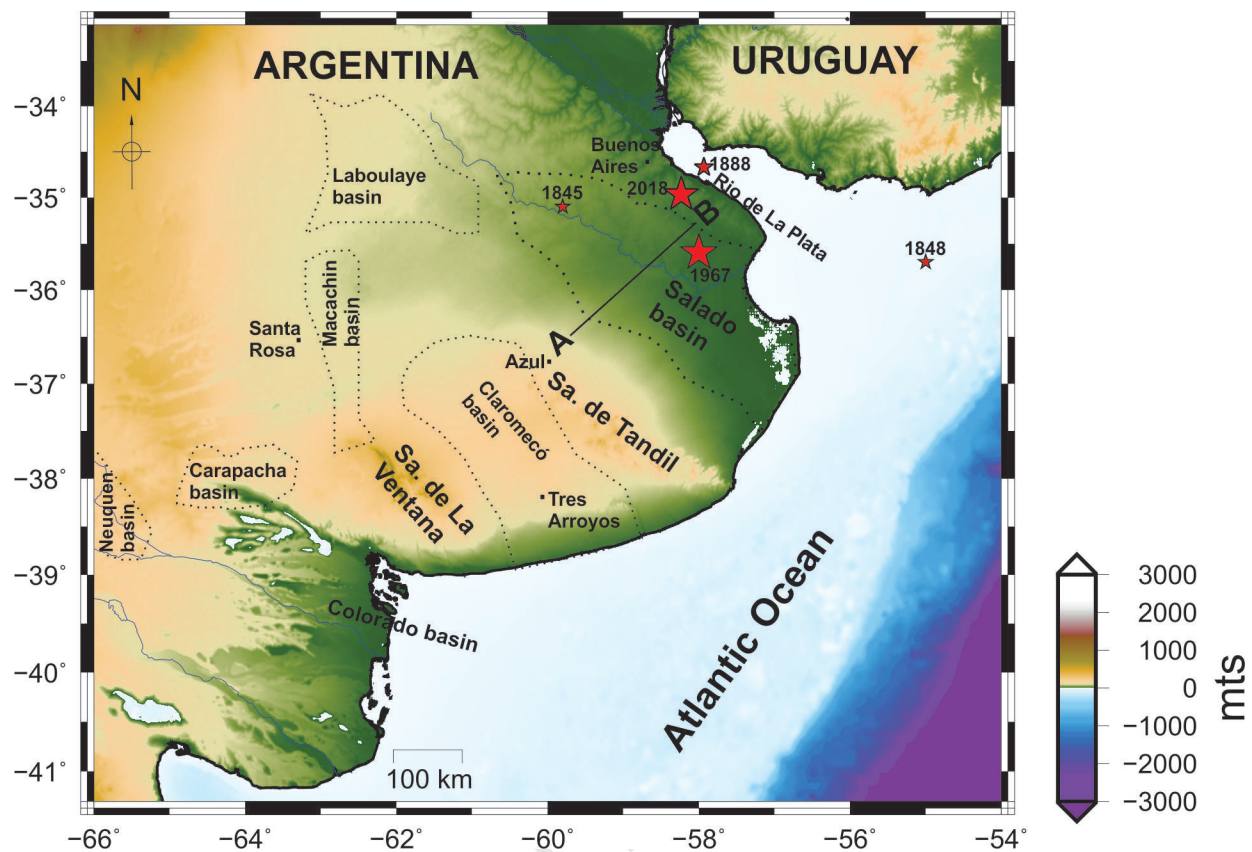
Figure 5: Cross-section for A-B in Figure 1. a) Moho model (Uieda and Barbosa, 2017). b) Sediment thickness (Crovetto et al., 2007), c) Digital terrain elevation model (Amante and Eakins, 2009) d) Isostatic residual anomaly obtained in this work.

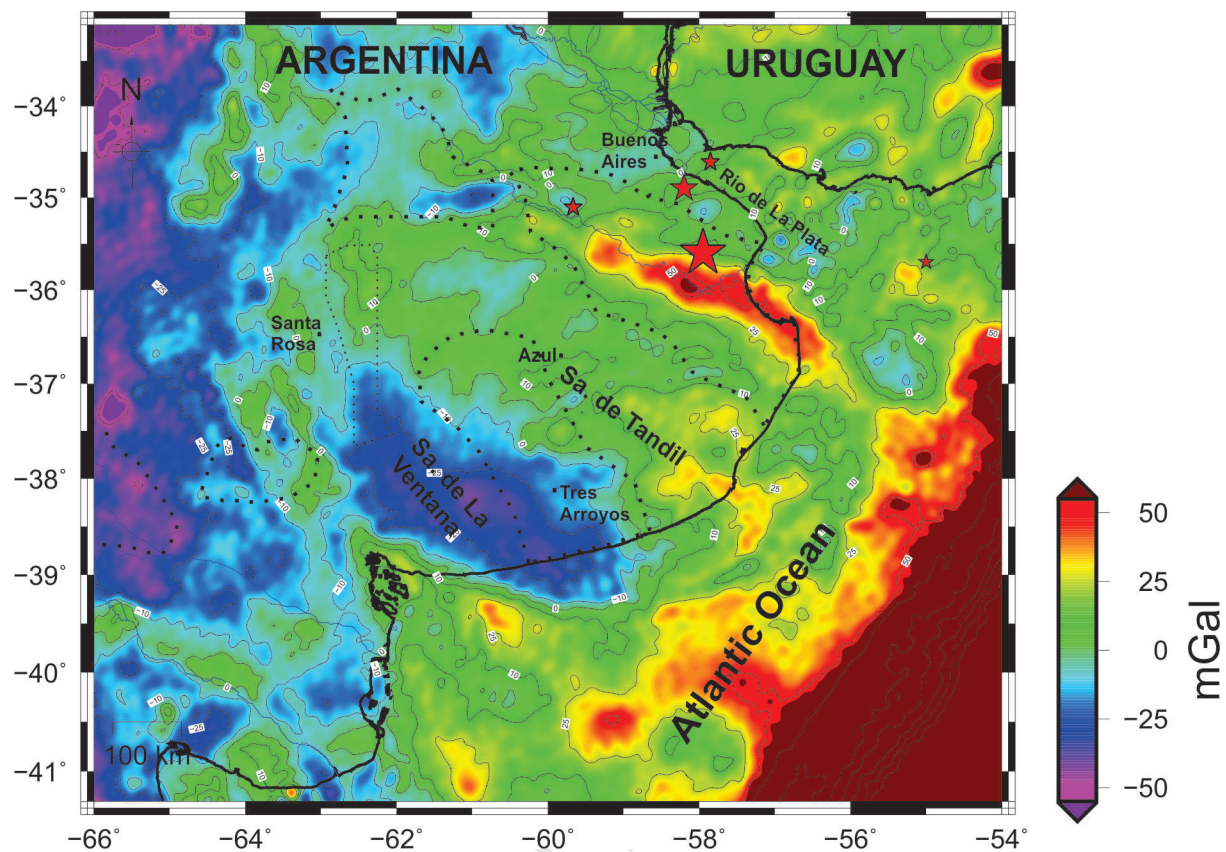
Figure 6: Cross-section through the crust through the Salado basin, which indicates the thickness of sediments, the anti-root under the basin and used densities

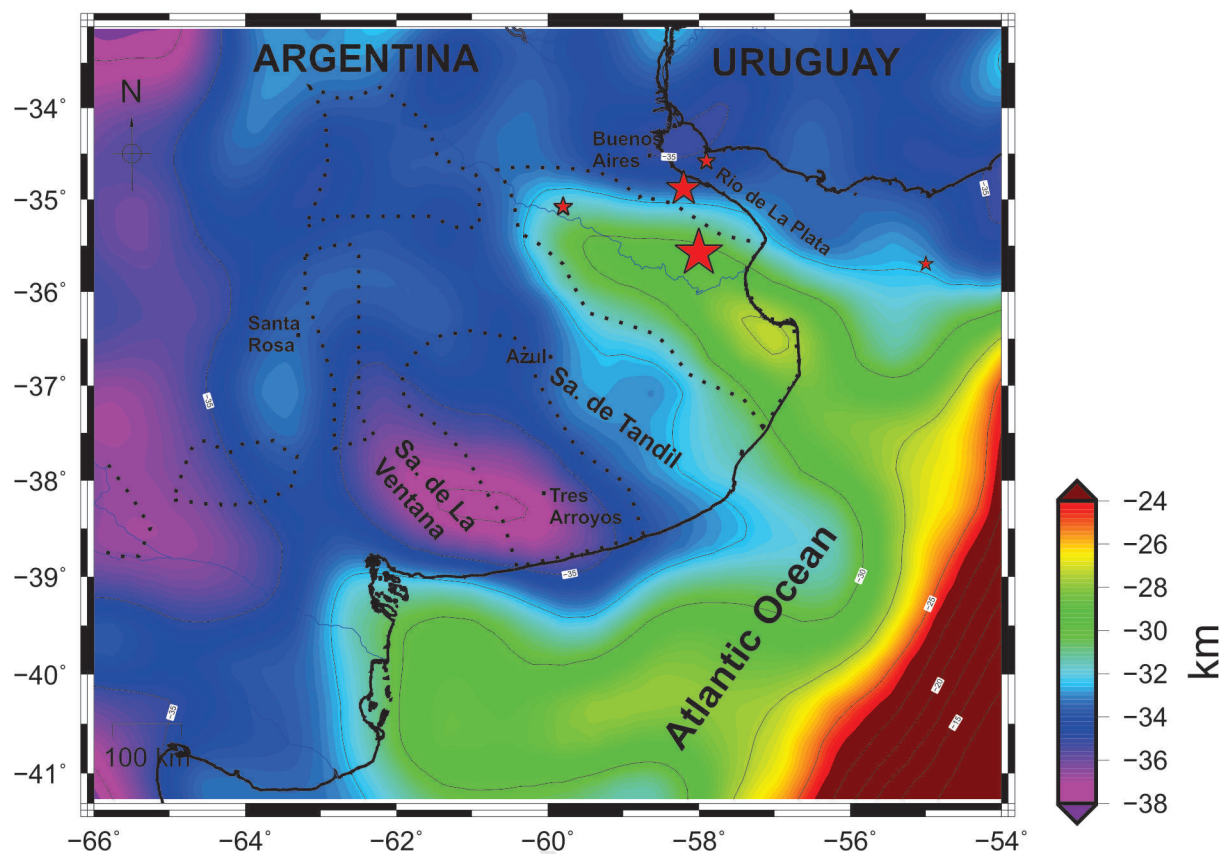
Figure 7: 3D model that integrates the different datasets presented in this work.

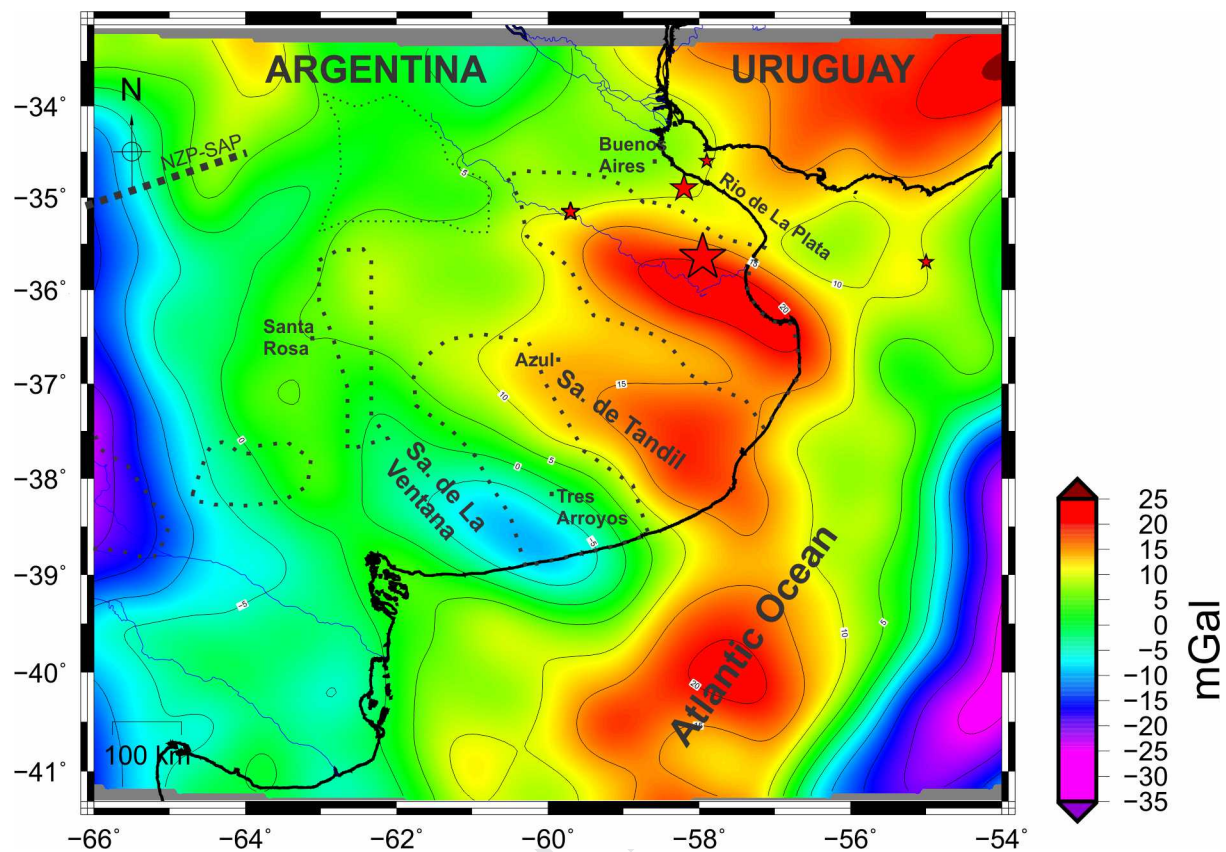
Table I: Historical and recent seismicity. Only 2018 earthquake location is used in the interpretation.

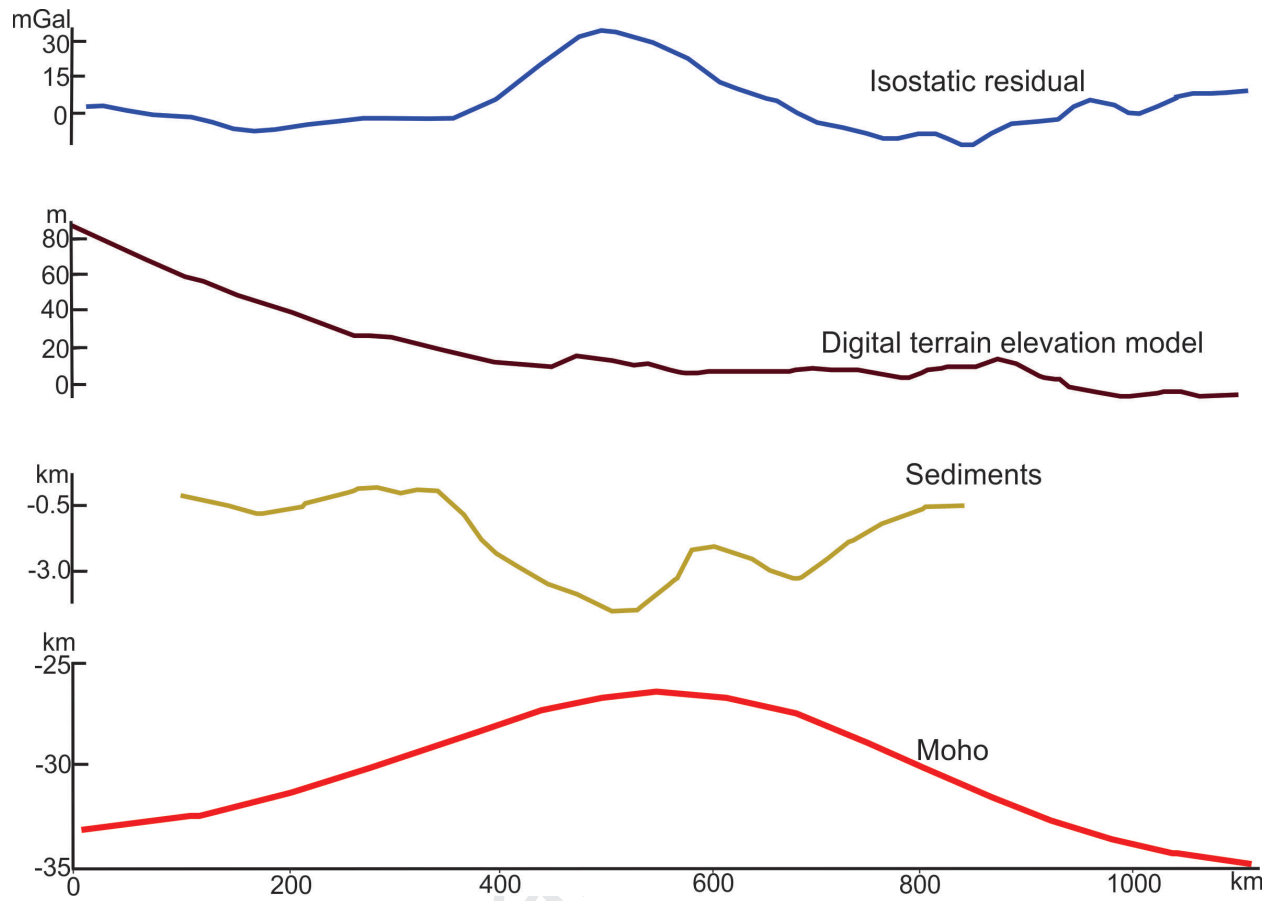
Date	Longitude (°)	Error (km)	Latitude (°)	Error (km)	Depth (km)	Magnitude	References
1845	-59,8	-	-35,1		30,00	-	CERESIS Catalog
1848	-55	-	-35,7		-	-	Benavidez 1998
1888	-57,9	-	-34,6		30,00	-	CERESIS Catalog
1967	-58,0	-	-35,6		33,00	5.0	CERESIS Catalog
1988	-52,7	-	-36,3		31,40	3,9	NEIC Catalog
2018	-58,2	±5.2	-34,9	±6.2	19±6	3,7	Venerdini et al., 2019

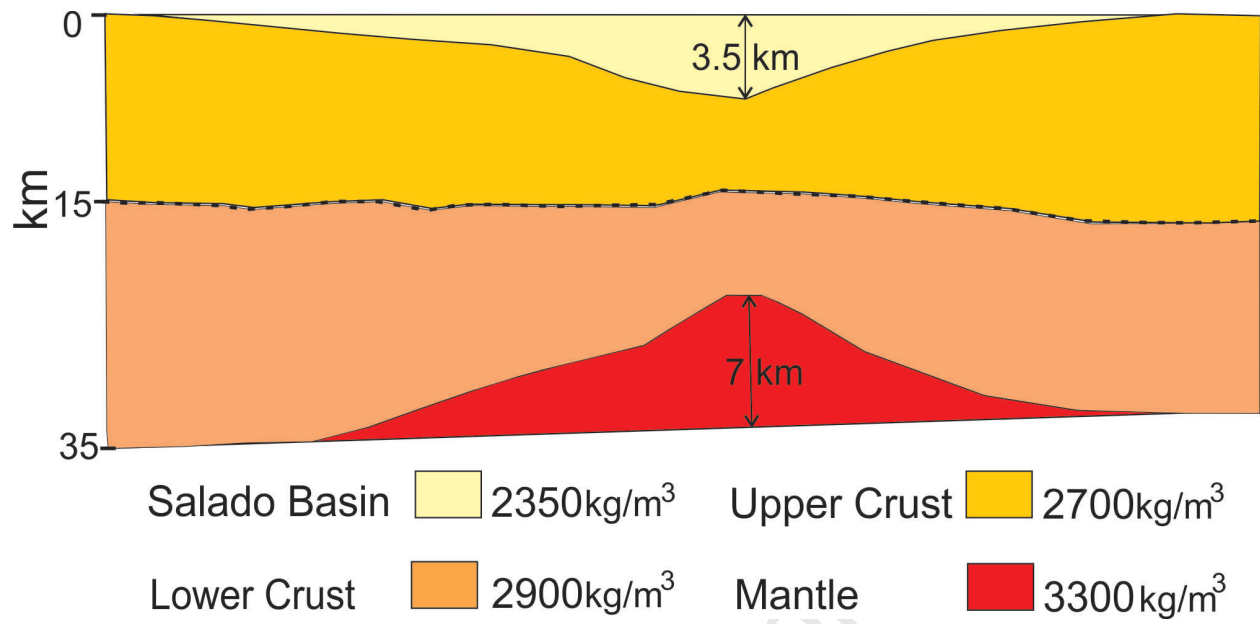


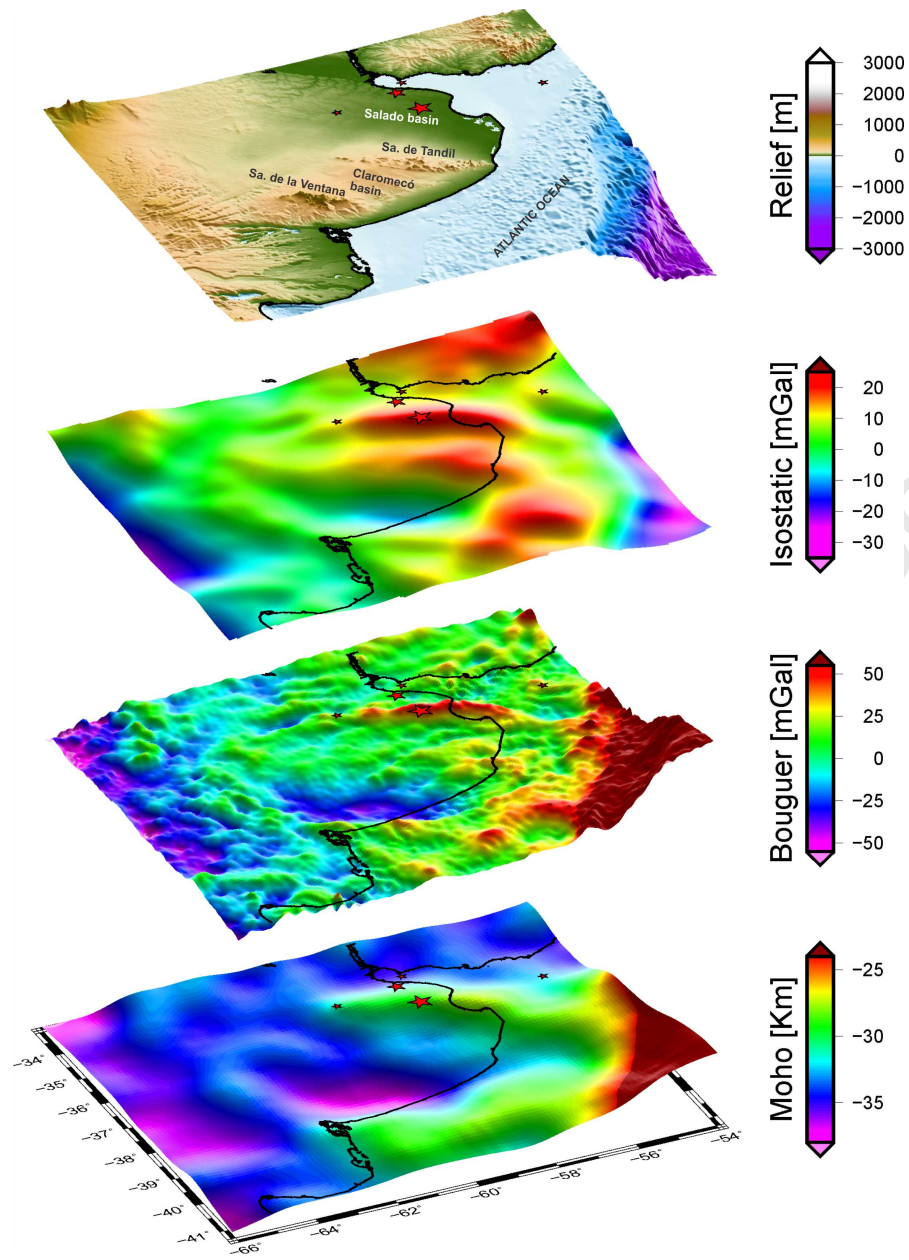












Significant crustal attenuation in Salado Basin

Positive gravimetric effect in Rio de la Plata Estuarine

Shallow seismic event located at basin edge probably associated with isostatic readjustment

Laura Godoy and Mario Gimenez conceived of the presented idea. Also, those authors developed the theory and performed the computations. Silvina Nacif interpreted seismological available data. Orlando Alvarez produce the final figures. Andres Folguera support the geological setting and contributed to the final manuscript.

Considering conflict of interest we refused the persons below

Dra. Patricia Alvarado

alvarado@unsj.edu.ar